Advances in Differential Equations and Control Processes 2025, 32(2), 3054.
https://doi.org/10.59400/adecp3054

Article

Generating directional attractors based on multiple subdivision

Baoxing Zhang[1,*], **Hongchan Zheng**[2], **Yuanyuan Xie**[3]

[1] College of Statistics and Mathematics, Hebei University of Economics and Business, Shijiazhuang 050061, China
[2] School of Mathematics and Statistics, Northwestern Polytechnical University, Xi'an 710072, China
[3] Institute of Science and Technology, Tianjin University of Finance and Economics, Tianjin 300222, China
* **Corresponding author:** Baoxing Zhang, baoxingzhang@hueb.edu.cn

CITATION

Zhang B, Zheng H, Xie Y. Advances in Differential Equations and Control Processes. 2025; 32(2): 3054. https://doi.org/10.59400/adecp3054

ARTICLE INFO

Received: 4 April 2025
Revised: 9 June 2025
Accepted: 24 June 2025
Available online: 30 June 2025

Abstract: This paper proposes a novel approach for generating directional controllable attractors through a multiple iterated function system architecture. Unlike conventional isotropic systems that exhibit uniform geometric properties in all directions, our approach generates attractors with controlled orientation features based on multiple anisotropic subdivision operators. Such attractors are useful in modeling real-world phenomena like natural scenes and biological systems. For the multiple iterated function system, we show the existence and uniqueness of the corresponding attractors. Then by giving two ways to control the whole iteration process, the attractors with different directions can be generated. The framework for generating directional attractors in this paper generalizes the existing subdivision-fractal connection by bridging the gap between isotropic fractal generation and practical anisotropic modeling. Several examples are given to illustrate these new directional attractors.

Keywords: Iterated function system; multiple iterated function system; multiple subdivision; iteration process control; directional attractors
MSC CLASSIFICATION: 35B41; 39B12

1. Introduction

Fractals have two geometric properties: they are self-similar and they are attractors. On the other hand, subdivision schemes are efficient tools to generate smooth surfaces, which are actually also attractors. Therefore, there is a deep connection between fractals and subdivision.

For such a connection, Schaefer et al. [1] first established the foundational relationship between self-similar fractals and classic stationary subdivision schemes. This seminar work spurred continuous subsequent works on this topic. For example, Levin et al. [2] generalized this connection and formalized the relationship between fractals and non-stationary subdivision schemes. Hu et al. [3] calculated the fractal dimension of curves generated by subdivision. Dyn et al. [4] further generalized these findings to the case of non-uniform subdivision schemes. For other references on the fractal-subdivision relationships, please refer to [5–10] and the references therein.

Yet, all of the above works focus on univariate or isotropic cases. Thus the corresponding attractors do not have directions. This limitation motivates our investigation into directional attractor generation. Such attractors actually appear more closer to nature with applications in natural scenes modeling [11] and also other fields like the works in [12–14]. Besides, this study intersects with emerging research trends, such as the interesting works in [15–17].

Our method comes from two insights: the connection between fractals and non-stationary subdivision and also the multiple subdivision schemes, which have several anisotropic subdivision operators and are capable of generating directional surfaces (See [18–21] and the references therein for more details). To generate the directional attractorFFs, we construct an iterated function system for each anisotropic subdivision operator of the multiple subdivision to derive a set of iterated function systems. These iterated function systems actually form a kind of multiple function system. Similar to the multiple subdivision, the multiple iterated function system chooses one iterated function system for each round of iteration [22]. In other words, the multiple iterated function system operates through path-dependent iterations within a hierarchical tree structure. For such a system, we show the existence and uniqueness of the attractor along each path of the tree. Besides, we give two ways to control the iteration process, which demonstrate the system's flexibility: one only by the path predetermination and the other by the modification of the iterated function systems. Several numerical examples are given to show the performance of the new multiple function systems and the corresponding directional attractors.

The rest of this paper is organized as follows. In Section 2, we recall some basic knowledge about subdivision and iterated function systems, which is needed in the rest of this paper. In Section 3, we construct an iterated function system based on an anisotropic subdivision operator to get a multiple function system and show the existence and uniqueness of the corresponding attractor along each path. Section 4 is devoted to present the ways to control the iteration process to generate directional attractors together with a discussion on the corresponding applications while Section 5 concludes this paper.

2. Preliminaries

In this section, we recall some basic notions and facts about subdivision and iterated function systems, which form the basis of this paper.

2.1. Subdivision

Let $l_0(\mathbb{Z}^2)$ denote the linear space of real-valued sequences with finite support indexed by $\mathbb{Z}^2$. Given an initial data sequence $\boldsymbol{q}^0 \in l_0(\mathbb{Z}^2)$, the subdivision $S_{\boldsymbol{a}}$ generates denser sequences from coarser sequences through the procedure,

$$\boldsymbol{q}^{k+1}(\boldsymbol{\alpha}) = (S_{\boldsymbol{a}}\boldsymbol{q}^k)(\boldsymbol{\alpha}) := \sum_{\boldsymbol{\beta}\in\mathbb{Z}^s} a(\boldsymbol{\alpha} - M\boldsymbol{\beta})q^k(\boldsymbol{\beta}), \quad \boldsymbol{\alpha} \in \mathbb{Z}^2 \tag{1}$$

where the 2×2 integer matrix M is the dilation matrix and $\boldsymbol{a} \in l_0(\mathbb{Z}^2)$ is the mask with finite support. With the mask $\boldsymbol{a}$, the corresponding subdivision matrix S can be given [1], with which, the subdivision procedure in Equation (1) is actually equivalent to the following iterattion process

$$\boldsymbol{q}^{k+1} = S\boldsymbol{q}^{k} \tag{2}$$

For the dilation matrix M, it is classified as isotropic if its eigenvalues satisfy $|\lambda| = |det(M)|^{1/2}$, otherwise M is an anisotropic one (see [23] for more details). This paper focuses on the subdivision operators with anisotropic dilation matrices, which are said to be the anisotropic subdivision operators in this paper. Besides, if the mask and the corresponding subdivision matrix depend on k, this subdivision is said to be a non-stationary subdivision.

Among all the subdivision schemes, only the multiple subdivision generates surfaces with directions [19]. Let $\{S_{\boldsymbol{a}_i}\}_{i=0}^{m}$ be a set of anisotropic subdivision operators. The corresponding multiple subdivision chooses one subdivision operator $S_{\boldsymbol{a}_i}$ for each round of subdivision. Let $\mathbb{Z}_m = \{0, \cdots, m-1\}$ with $m \in \mathbb{Z}_+$, then the way to choose the subdivision operators for each step of subdivision can be characterized with an additional parameter $\boldsymbol{\epsilon} = (\epsilon_1, \epsilon_2, \cdots) \in \mathbb{Z}_m^{\infty}$ with elements in $\mathbb{Z}_m$. Let $\boldsymbol{\epsilon}^n = (\epsilon_1, \cdots, \epsilon_n)$, $\epsilon_i \in \mathbb{Z}_m$, then we have the multiple subdivision operator $S_{\boldsymbol{a}_{\boldsymbol{\epsilon}}} = S_{\boldsymbol{a}_{\epsilon_1}} \circ \cdots \circ S_{\boldsymbol{a}_{\epsilon_n}}$. The multiple subdivision can be arranged in a tree structure as shown in **Figure 1**, which presents the binary ($m = 2$) case [18].

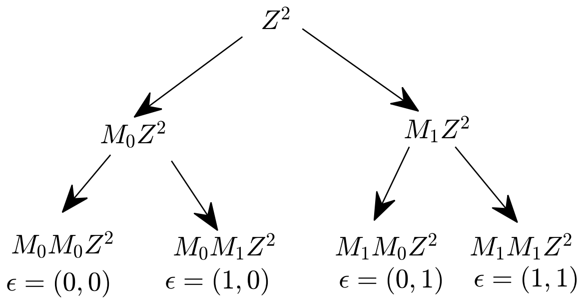

Figure 1. The binary tree (with $m = 2$) structure with refinement scheme.

For simplicity, we consider the multiple subdivision $S_{\boldsymbol{a}_{\boldsymbol{\epsilon}}}$ with anisotropic subdivision operators $S_{\boldsymbol{a}_0}$ and $S_{\boldsymbol{a}_1}$. The dilation matrix of $S_{\boldsymbol{a}_0}$ is a diagonal matrix M_0 and the dilation matrix of $S_{\boldsymbol{a}_1}$ is

$$M_1 = UM_0V$$

where U and V are unimodular matrices. Suppose $|M_0| = n$, then $|M_1| = n$. These two subdivision operators satisfy

$$S_{\boldsymbol{a}_1} = D_U S_{\boldsymbol{a}_0} D_V \tag{3}$$

Equation (3) implies the geometry of the subdivision operator $S_{\boldsymbol{a}_1}$: a shearing by D_V is applied to the data sequence first and then the subdivision operator $S_{\boldsymbol{a}_0}$ refines them in the sheared direction. After that, the additional application of the shearing by D_U is applied again to the refined data sequence. Such a process leads to limit functions which are sheared versions of that of $S_{\boldsymbol{a}_0}$ and the amount of shearing depends on when and how often $S_{\boldsymbol{a}_1}$ is applied [18]. Here, the shearing operator D_V acts as

$$D_V \boldsymbol{q}^0(\cdot) = \boldsymbol{q}^0(V\cdot) \tag{4}$$

where $V = \begin{pmatrix} 1 & k \\ 0 & 1 \end{pmatrix}$ with $k \in \mathbb{Z}$.

2.2. Iterated function systems

Now we recall iterated function systems over the complete metric space (X, d). A function $f : X \to X$ is said to be contractive if the corresponding Lipschitz constant

$$Lip(f) = \sup_{x,y \in X, x \neq y} \frac{d(f(x), f(y))}{d(x, y)} < 1$$

Let $\mathbb{H}(X)$ be the collection of all nonvoid compact subsets of X. Then $\mathbb{H}(X)$ is a complete metric space endowed with the Hausdorff metric

$$h(B, C) = \max\{d(B, C), d(C, B)\}$$

where $d(B, C) = \sup_{b \in B} d(b, C) = \sup_{b \in B} \inf_{c \in C} d(b, c)$ [2].

Let $\mathcal{F} = \{X; f_i : i = 1, .., s\}$ be a set of contractive maps. For $B \in \mathbb{H}(X)$, let

$$\mathcal{F}(B) := \cup_{f \in \mathcal{F}} f(B)$$

where $f(B) := \{f(b) : b \in B\}$ with the corresponding Lipschitz constant

$$L_{\mathcal{F}} = \max_{i=1,\ldots,s} Lip(f_i) \tag{5}$$

A set A is said to be an attractor of the iterated function system $\mathcal{F}$ if $\mathcal{F}(A) = A$, which can be generated by the iteration procedure $A_{i+1} = \mathcal{F}(A_i)$ with an initial set A_0.

Based on one subdivision operator $S_{\boldsymbol{a}}$, Schaefer et al. [1] construct the iterated function systems with the contractive functions

$$f_i(A) = AP^{-1}S_iP, \quad A \subset Q^{n-1}$$

Here, Q^{n-1} is the $n - 1$ dimensional hyperplane with points of the form $(x_1, \cdots, x_{n-1}, 1)$, the $n \times n$ matrix P is constructed with the n points in $\mathbb{R}^m$ satisfying the following conditions: the first m columns are the n given control points in $\mathbb{R}^m$; the last column is a column of $1's$ and the rest columns are such that the matrix P is non-singular. The matrix S_i with the same size as P^0 is the sub-subdivision matrixo btained by breaking the matrix S in Equation (13) into multiple $n \times n$ submatrices. In this way, it can be seen that with $X = P$, the corresponding attractor is just the limit surface of the subdivision scheme [1].

Given two subdivision operators $S_{\boldsymbol{a}_0}$ and $S_{\boldsymbol{a}_1}$, following Schaefer [1], we derive two iterated function systems as

$$\mathcal{F}_0 = \{f_{0,1}, \cdots, f_{0,n_0}\}, \quad \mathcal{F}_1 = \{f_{1,1}, \cdots, f_{1,n_1}\}$$

Then we get a multiple function system $\mathcal{F}_{\boldsymbol{\epsilon}}$, which we denote by $\mathcal{F}_{\boldsymbol{\epsilon}} = \{\mathcal{F}_0, \mathcal{F}_1\}$ with $\boldsymbol{\epsilon} = (\epsilon_1, \epsilon_2, \cdots) \in \mathbb{Z}_2^{\infty}$ [22]. This multiple function system chooses one iterated function system for each step of iteration, i.e.

$$\mathcal{F}_{\boldsymbol{\epsilon}} = \mathcal{F}_{\epsilon_1} \circ \mathcal{F}_{\epsilon_2} \circ \cdots \mathcal{F}_{\epsilon_k} \circ \cdots \tag{6}$$

Such a multiple function system can be arranged in a tree structure as shown in **Figure 2**.

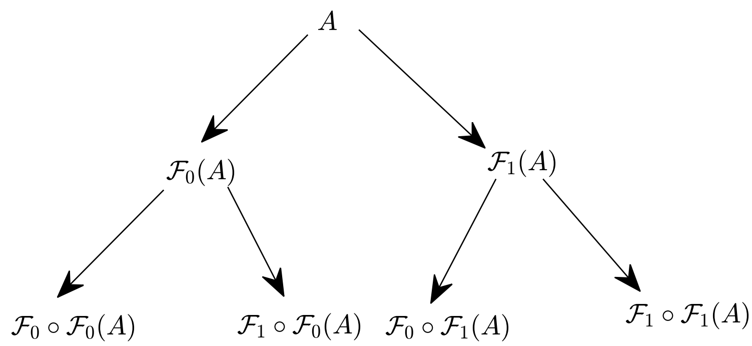

Figure 2. The binary tree structure of the multiple function system $\mathcal{F}_{\boldsymbol{\epsilon}}$ with the initial set A.

For such a tree, a path $\boldsymbol{\epsilon} \in \mathbb{Z}_2^{\infty}$ characterizes the choice of the iterated function system for each time of iteration. Therefore, along different paths, we obtain different attractors. For a given path $\boldsymbol{\epsilon} = (\epsilon_1, \epsilon_2, \cdots, \epsilon_k, \cdots)$, the corresponding iteration process in Equation (6) can also be characterized in a mapping tree structure as in **Figure 3**.

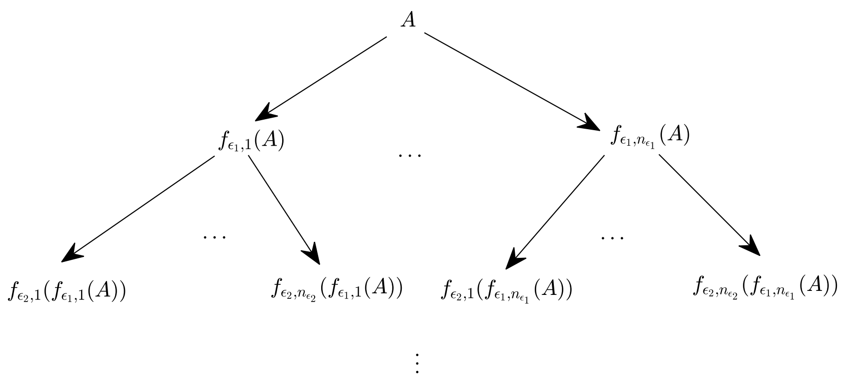

Figure 3. The mapping tree structure of the multiple function system $\mathcal{F}_{\boldsymbol{\epsilon}}$ with a given $\boldsymbol{\epsilon} \in \mathbb{Z}_2^{\infty}$ and the initial set A.

3. Multiple iterated function systems based on multiple subdivision

In this section, we construct the desired multiple iterated function systems and show the existence and uniqueness of the corresponding attractors.

3.1. Multiple function systems with directions

While Schaefer's framework recalled in Section 2.2 provides a simple and efficient method to derive iterated function systems from stationary subdivision operators, it is not suitable for the multiple subdivision due to the shearing operators in Section 2.1. For this, we present a novel approach to construct directional controllable multiple iterated function systems based on the multiple subdivision.

For the multiple subdivision $S_{\boldsymbol{a}_\epsilon}$ with the anisotropic subdivision operators $S_{\boldsymbol{a}_0}$ and $S_{\boldsymbol{a}_1}$, we first construct the iterated function system for $S_{\boldsymbol{a}_0}$. In fact, for the i-th round of iteration with $i \leq k$ ($k \in \mathbb{Z}_+$), we define

$$f_{0,r}^{[i]}(A) = \begin{cases} AS_r, & i = 1, \cdots, k-1, \\ AS_r p^0, & i = k, \end{cases} \qquad r = 1, \cdots, n_0 \tag{7}$$

Here, A is the initial set for the iteration process chosen from the set

$$K^{n-1} := \{(x_1, x_2, \cdots, x_n) : \sum_{i=1}^{n} x_i = 1\}$$

$p^0 \in \mathbb{R}^{n\times 3}$ is the matrix with rows being the n initial control points in $\mathbb{R}^3$ and S_r ($r = 1, \cdots, n_0$) are the $n \times n$ sub-subdivision matrices of $S_{\boldsymbol{a}_0}$. Then the iterated function system for the subdivision operator $S_{\boldsymbol{a}_0}$ is

$$\mathcal{F}_0^{[k]} = \{f_{0,1}^{[k]}, \cdots, f_{0,n_0}^{[k]}\}$$

After k rounds of iterations using this iterated function system, we get the set

$$\mathcal{F}_0^{[k]} \circ \cdots \circ \mathcal{F}_0^{[1]}(A) = \bigcup_{i_1,\cdots,i_k \in \{1,\cdots,n_0\}} AS_{i_k} \cdots S_{i_1} p^0$$

As for the subdivision operator $S_{\boldsymbol{a}_1}$, as shown in Subsection 2.2, it incorporates shearing operators. Therefore, for the i-th round of iteration with $i \leq k$ ($k \in \mathbb{Z}_+$), define

$$f_{1,r}^{[i]}(A) = \begin{cases} AD_U S_r D_V, & i = 1, \cdots, k-1, \\ AD_U S_r D_V(p^0), & i = k, \end{cases} \qquad r = 1, \cdots, n_1 \tag{8}$$

Therefore, the corresponding iterated function system is $\mathcal{F}_1^{[k]} = \{f_{1,1}^{[k]} \cdots, f_{1,n_1}^{[k]}\}$ and after k rounds of iterations using this multiple function system, we get the set

$$\mathcal{F}_1^{[k]} \circ \cdots \circ \mathcal{F}_1^{[1]}(A) = \bigcup_{i_1,\cdots,i_k \in \{1,\cdots,n_1\}} AD_U S_{i_k} D_V \cdots D_U S_{i_1} D_V(p^0)$$

Now based on the two iterative function systems, the desired multiple function system for the multiple subdivision operator $S_{\boldsymbol{a}_{\boldsymbol{\epsilon}}}$ is $\mathcal{F}_{\boldsymbol{\epsilon}}^{[k]} = \{\mathcal{F}_0^{[k]}, \mathcal{F}_1^{[k]}\}$ with $\boldsymbol{\epsilon} \in \mathbb{Z}_2^\infty$. For such a multiple function system, we choose one iterated function system for each step of iteration. In other words, with the given sequence $\boldsymbol{\epsilon} = (\epsilon_1, \epsilon_2, \cdots, \epsilon_k) \in \mathbb{Z}_2^k$, the iteration process can be characterized as:

$$\mathcal{F}_{\boldsymbol{\epsilon}}^{[k]} = \mathcal{F}_{\epsilon_k}^{[k]} \circ \cdots \circ \mathcal{F}_{\epsilon_1}^{[1]}$$

and thus the corresponding generated set initialized with A is actually the following one

$$\mathcal{F}_{\epsilon_k}^{[k]} \circ \cdots \circ \mathcal{F}_{\epsilon_1}^{[1]}(A) = \bigcup_{i_j \in \{1,\cdots,n_{\epsilon_j}\}, j=1,\cdots,k} f_{\epsilon_k,i_k}^{[k]} \circ \cdots \circ f_{\epsilon_1,i_1}^{[1]}(A) \tag{9}$$

Let D_{U_1} and D_{V_1} denote the shearing operators in Equation (8) and D_{U_0} and D_{V_0} the operators without shearing, which means that $D_{U_0}\boldsymbol{p}^0 = D_{V_0}\boldsymbol{p}^0 = \boldsymbol{p}^0$, then the iteration operators in Equations (7) and (8) can be rewritten as

$$f_{0,r}^{[i]}(A) = \begin{cases} AD_{U_0}S_rD_{V_0}, & i = 1,\cdots,k-1, \\ AD_{U_0}S_rD_{V_0}(p^0), & i = k, \end{cases} \qquad r = 1,\cdots,n_0$$

and

$$f_{1,r}^{[i]}(A) = \begin{cases} AD_{U_1}S_rD_{V_1}, & i = 1,\cdots,k-1, \\ AD_{U_1}S_rD_{V_1}(p^0), & i = k, \end{cases} \qquad r = 1,\cdots,n_1$$

In this way, the set in Equation (9) can be rewritten as

$$\mathcal{F}_{\epsilon_k}^{[k]} \circ \cdots \circ \mathcal{F}_{\epsilon_1}^{[1]}(A) = \bigcup_{i_j \in \{1,\cdots,n_{\epsilon_j}\}, j=1,\cdots,k} AD_{U_{\epsilon_k}}S_{i_k}D_{V_{\epsilon_k}} \cdots D_{U_{\epsilon_1}}S_{i_1}D_{V_{\epsilon_1}}p^0$$

3.2. Attractors of the multiple function systems with directions

Now we discuss the existence and uniqueness of the attractors of the multiple function system constructed in Subsection 3.1, which is actually stated in the following result.

Theorem 1. *Given a convergent multiple subdivision $S_{\boldsymbol{a}_{\boldsymbol{\epsilon}}}$ with the anisotropic subdivision operators $S_{\boldsymbol{a}_0}$ and $S_{\boldsymbol{a}_1}$ and the initial point matrix $\mathrm{p}^0 \in \mathbb{R}^{n\times 3}$, let the corresponding multiple function system be $\mathcal{F}_{\boldsymbol{\epsilon}}^{[k]} = \{\mathcal{F}_0^{[k]}, \mathcal{F}_1^{[k]}\}$. Then for each $\boldsymbol{\epsilon} = (\epsilon_1, \epsilon_2, \cdots, \epsilon_k) \in \mathbb{Z}_2^k$, as k tends to infinity, $\mathcal{F}_{\epsilon_k}^{[k]} \circ \cdots \circ \mathcal{F}_{\epsilon_1}^{[1]}(A)$ converges to a unique attractor with $A \subset K^{n-1}$, which coincides with the limit surface of $S_{\boldsymbol{a}_{\boldsymbol{\epsilon}}}$ starting from the initial points in p^0.*

Proof. Since the multiple subdivision $S_{\boldsymbol{a}_{\boldsymbol{\epsilon}}}$ converges, it follows that for $A \subset K^{n-1}$, with $\boldsymbol{\epsilon} = (\epsilon_1, \epsilon_2, \cdots, \epsilon_k) \in \mathbb{Z}_2^k$, we get the set,

$$\begin{aligned} \mathcal{F}_{\epsilon_k}^{[k]} \circ \cdots \circ \mathcal{F}_{\epsilon_1}^{[1]}(A) &= \bigcup_{i_j \in \{1,\cdots,n_{\epsilon_j}\}, j=1,\cdots,k} AD_{U_{\epsilon_k}}S_{i_k}D_{V_{\epsilon_k}} \cdots D_{U_1}S_{i_1}D_{V_1}p^0 \\ &= A \bigcup_{i_j \in \{1,\cdots,n_{\epsilon_j}\}, j=1,\cdots,k} D_{U_{\epsilon_k}}S_{i_k}D_{V_{\epsilon_k}} \cdots D_{U_1}S_{i_1}D_{V_1}p^0 \end{aligned} \tag{10}$$

Since $S_{\boldsymbol{a}_{\boldsymbol{\epsilon}}}$ converges, $\bigcup_{i_j \in \{1,\cdots,n_{\epsilon_j}\}, j=1,\cdots,k} D_{U_{\epsilon_k}}S_{i_k}D_{V_{\epsilon_k}} \cdots D_{U_1}S_{i_1}D_{V_1}p^0$ is actually the set obtained using the multiple subdivision $S_{\boldsymbol{a}_{\boldsymbol{\epsilon}}}$ with the same $\boldsymbol{\epsilon}$. Thus, $\mathcal{F}_{\epsilon_k}^{[k]} \circ \cdots \circ \mathcal{F}_{\epsilon_1}^{[1]}(A)$ converges as k tends to infinity due to the convergence of $S_{\boldsymbol{a}_{\boldsymbol{\epsilon}}}$.

Now we show that certain path of this multiple function system initialized with an arbitrary set $A \subset K^{n-1}$ converges to the same attractor. In fact, since the multiple subdivision $S_{\boldsymbol{a}_{\boldsymbol{\epsilon}}}$ converges, for a given $\boldsymbol{\epsilon} \in \mathbb{Z}_2^{\infty}$, let $\boldsymbol{\eta} = (i_1, \cdots, i_k, \cdots)$ denote the path of the corresponding mapping tree structure of $\mathcal{F}_{\boldsymbol{\epsilon}}^{[k]}$ in **Figure 3**. Then along a certain path η, it can be seen that the limit of the set $AD_{U_{\epsilon_k}} S_{i_k} D_{V_{\epsilon_k}} \cdots D_{U_1} S_{i_1} D_{V_1} p^0$ in Equation (10) is $A\boldsymbol{q}$, where $\boldsymbol{q}$ is a vector of n identical points, i.e.

$$\lim_{k\to\infty} AD_{U_{\epsilon_k}} S_{i_k} D_{V_{\epsilon_k}} \cdots D_{U_1} S_{i_1} D_{V_1} p^0 = A\boldsymbol{q} = A \begin{pmatrix} q_{\boldsymbol{\eta}} \\ \vdots \\ q_{\boldsymbol{\eta}} \end{pmatrix}$$

with $q_{\boldsymbol{\eta}}$ being the point in $\mathbb{R}^3$. Since $A \subset K^{n-1}$, we get that the limit is actually $A\boldsymbol{q} = q_{\boldsymbol{\eta}}$. Thus, we have

$$\lim_{k\to\infty} \mathcal{F}_{\epsilon_k} \circ \cdots \mathcal{F}_{\epsilon_1}(A) = \bigcup_{\boldsymbol{\eta}} q_{\boldsymbol{\eta}},$$

which is the limit generated by the multiple subdivision $S_{\boldsymbol{a}_{\boldsymbol{\epsilon}}}$ with the same $\boldsymbol{\epsilon}$ $\square$.

4. Generating directional attractors by controlling the iteration process

Now we try to use the new multiple function system obtained in Section 3 to generate directional attractors and discuss the corresponding applications. To this purpose, we give two ways to control the iteration process: path-dependent selection and shear operator modulation.

4.1. Directional attractors based on path-selection

Now we use the multiple function system in Section 3 to generate directional attractors by controlling the paths.

In fact, the multiple function system inherently generates directional attractors by path-selection. Besides, for the multiple function system $\mathcal{F}_{\boldsymbol{\epsilon}}^{[k]} = \{\mathcal{F}_0^{[k]}, \mathcal{F}_1^{[k]}\}$, we can also modify it by deleting some iterated functions from $\mathcal{F}_0^{[k]}$ or $\mathcal{F}_1^{[k]}$ so that regular or irregular fractals [24] can be obtained [22]. For such a modified multiple function system, along a certain path, it still converges to a unique attractor.

Now we give a concrete example to show the performance of this approach.

Example 1. *Let*

$$M_0 = \begin{pmatrix} 4 & 0 \\ 0 & 2 \end{pmatrix}, \qquad M_1 = \begin{pmatrix} 4 & -4 \\ 0 & 2 \end{pmatrix},$$

be two dilation matrices, which satisfies $M_1 = V^{-1} M_0 V$ *with* $V = \begin{pmatrix} 1 & -2 \\ 0 & 1 \end{pmatrix}$. *Let the binary* 2*-point B-spline subdivision mask be denoted as* $\boldsymbol{b}_0 = \{\frac{1}{2}, 1, \frac{1}{2}\}$ *and let* $\tilde{\boldsymbol{b}}_0$ *be defined as* $\tilde{b}(i) = \sum_k b_0(k) b_0(i-2k)$. *Then the subdivision operator* $S_{\boldsymbol{a}_0}$ *with the dilation matrix* M_0 *and the mask* $\boldsymbol{a}_0 = \tilde{\boldsymbol{b}}_0 \otimes \boldsymbol{b}_0$ *can be obtained. Accordingly, the subdivision operator* $S_{\boldsymbol{a}_1}$ *with the dilation matrix* M_1 *and the mask* $\boldsymbol{a}_1 = \boldsymbol{a}_0(V\cdot)$ *can* *also be derived (See Lemma* 4.15 *in [18]).*

Now we give the 4×3 initial point matrix as

$$p^0 = \begin{pmatrix} 0 & 0 & 0 \\ 1 & 0 & 0 \\ 1 & 1 & 0 \\ 0 & 1 & 0 \end{pmatrix} \tag{11}$$

and the corresponding eight sub-subdivision matrices of $S_{\boldsymbol{a}_0}$ as follows,

$$S_1 = \begin{pmatrix} 1 & 0 & 0 & 0 \\ \frac{3}{4} & \frac{1}{4} & 0 & 0 \\ \frac{3}{8} & \frac{1}{8} & \frac{1}{8} & \frac{3}{8} \\ \frac{1}{2} & 0 & 0 & \frac{1}{2} \end{pmatrix}, \quad S_2 = \begin{pmatrix} \frac{3}{4} & \frac{1}{4} & 0 & 0 \\ \frac{1}{2} & \frac{1}{2} & 0 & 0 \\ \frac{1}{4} & \frac{1}{4} & \frac{1}{4} & \frac{1}{4} \\ \frac{3}{8} & \frac{1}{8} & \frac{1}{8} & \frac{3}{8} \end{pmatrix}, \quad S_3 = \begin{pmatrix} \frac{1}{2} & \frac{1}{2} & 0 & 0 \\ \frac{1}{4} & \frac{3}{4} & 0 & 0 \\ \frac{1}{8} & \frac{3}{8} & \frac{3}{8} & \frac{1}{8} \\ \frac{1}{4} & \frac{1}{4} & \frac{1}{4} & \frac{1}{4} \end{pmatrix},$$

$$S_4 = \begin{pmatrix} \frac{1}{4} & \frac{3}{4} & 0 & 0 \\ 0 & 1 & 0 & 0 \\ 0 & \frac{1}{2} & \frac{1}{2} & 0 \\ \frac{1}{8} & \frac{3}{8} & \frac{3}{8} & \frac{1}{8} \end{pmatrix}, \quad S_5 = \begin{pmatrix} \frac{1}{2} & 0 & 0 & \frac{1}{2} \\ \frac{3}{8} & \frac{1}{8} & \frac{1}{8} & \frac{3}{8} \\ 0 & 0 & \frac{1}{4} & \frac{3}{4} \\ 0 & 0 & 0 & 1 \end{pmatrix}, \quad S_6 = \begin{pmatrix} \frac{3}{8} & \frac{1}{8} & \frac{1}{8} & \frac{3}{8} \\ \frac{1}{4} & \frac{1}{4} & \frac{1}{4} & \frac{1}{4} \\ 0 & 0 & \frac{1}{2} & \frac{1}{2} \\ 0 & 0 & \frac{1}{4} & \frac{3}{4} \end{pmatrix},$$

$$S_7 = \begin{pmatrix} \frac{1}{4} & \frac{1}{4} & \frac{1}{4} & \frac{1}{4} \\ \frac{1}{8} & \frac{3}{8} & \frac{3}{8} & \frac{1}{8} \\ 0 & 0 & \frac{3}{4} & \frac{1}{4} \\ 0 & 0 & \frac{1}{2} & \frac{1}{2} \end{pmatrix}, \quad S_8 = \begin{pmatrix} \frac{1}{8} & \frac{3}{8} & \frac{3}{8} & \frac{1}{8} \\ 0 & \frac{1}{2} & \frac{1}{2} & 0 \\ 0 & 0 & 1 & 0 \\ 0 & 0 & \frac{3}{4} & \frac{1}{4} \end{pmatrix}.$$

Then we get two multiple function systems $\mathcal{F}_{\boldsymbol{\epsilon}}^{[k]} = \{\mathcal{F}_0^{[k]}, \mathcal{F}_1^{[k]}\}$ and $\bar{\mathcal{F}}_{\boldsymbol{\epsilon}}^{[k]} = \{\bar{\mathcal{F}}_0^{[k]}, \mathcal{F}_1^{[k]}\}$, with

$$\mathcal{F}_0^{[k]} = \{f_{0,i}^{[k]}, i = 1, \cdots, 8\}, \mathcal{F}_1^{[k]} = \{f_{1,i}^{[k]}, i = 1, \cdots, 8\}, \bar{\mathcal{F}}_0^{[k]} = \{f_{0,i}^{[k]}, i = 3, \cdots, 8\}.$$

Here,

$$f_{0,r}^{[i]}(A) = \begin{cases} AS_r, & i = 1, \cdots, k-1, \\ AS_r p^0, & i = k, \end{cases} \qquad r = 1, \cdots, 8 \tag{12}$$

and

$$f_{1,r}^{[i]}(A) = \begin{cases} AD_{V^{-1}} S_r D_V, & i = 1, \cdots, k-1, \\ AD_{V^{-1}} S_r D_V(p^0), & i = k, \end{cases} \qquad r = 1, \cdots, 8$$

Figure 4 shows the sets obtained using these two multiple function systems with different $\boldsymbol{\epsilon}$.

Figure 4 confirms that, the multiple function system obtained in Section 3 is indeed able to generate attractors with directions through path-selection. But all parts of the attractors keep the same direction, which means that path selection dictates global direction patterns.

Figure 4. Sets generated by the multiple function systems $\mathcal{F}_{\boldsymbol{\epsilon}}^{[k]}$ with $\boldsymbol{\epsilon} = (0,0,0,0,0)$ (left), $(1,0,0,0,0)$ (middle) and $\bar{\mathcal{F}}_{\boldsymbol{\epsilon}}^{[k]}$ with $\boldsymbol{\epsilon} = (0,0,0,0,0)$ (right) using p^0 in Equation (11).

4.2. Directional fractals based on shear operator modulation

To achieve localized directional variation, now we give a new way to control the iteration process by enhancing the multiple iterated function systems with position-dependent shear operators. For this, we need to slightly modify the multiple function system in Section 3.

Note that the obtained attractors have directions due to the use of the iterated function system $\mathcal{F}_1^{[k]}$, which contains the shearing operators. Besides, all the iterated functions in $\mathcal{F}_1^{[k]}$ contain the same shearing operators, which actually leads to the attractors with global direction patterns. Moreover, the effect of the shearing operator D_V in Equation (4) can be seen as moving a point along the x-coordinate, which can be seen from Example 1.

Therefore, we mainly modify $\mathcal{F}_1^{[k]}$ so that different iterated functions have different shearing operators. Specifically speaking, we define

$$f_{1,r,s,t,p,q}^{[i]}(A) = \begin{cases} AD_{V_{s,t}}S_rD_{V_{p,q}}, & i = 1,\cdots,k-1, \\ AD_{V_{s,t}}S_rD_{V_{p,q}}(p^0), & i = k, \end{cases} \quad r = 1,\cdots,n_1 \tag{13}$$

Here, similar to the shearing operator D_V, the operator $D_{V_{p,q}}$ moves a point on the lower edge p units and a point on the upper edge q units, as shown in **Figure 5** with the case $D_{V_{3,4}}$. In fact, when $q = kp$, the effect of $D_{V_{p,q}}$ is the same with that of D_V in Equation (4). In this way, we get a new iterated function system, which we still denote by $\mathcal{F}_1^k$, and a new multiple function system, which we still denote by $\mathcal{F}_{\boldsymbol{\epsilon}}^{[k]}$.

When using this modified multiple function system to generate attractors, for simplicity, we only apply the new iterated function system $\mathcal{F}_1^k$ finite times in the whole iteration process and use $\mathcal{F}_0^{[k]}$ for the rest rounds of iterations. In this way, the existence and uniqueness of the corresponding attractors can be guaranteed by Theorem 1, as shown in the following result.

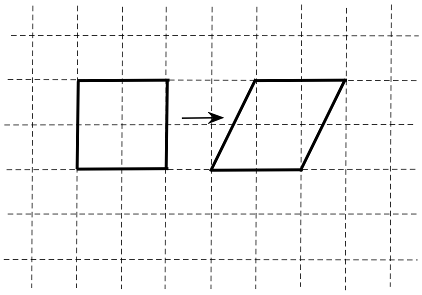

Figure 5. The effect of the new shearing operator $D_{V_{3,4}}$.

Corollary 1. *Let* $\mathcal{F}_{\boldsymbol{\epsilon}}^{[k]} = \{\mathcal{F}_0^{[k]}, \mathcal{F}_1^{[k]}\}$ *denote the modified multiple function system. Then along the path* $\boldsymbol{\epsilon} = (\epsilon_1, \cdots, \epsilon_k, 0, \cdots)$, $\epsilon_1, \cdots, \epsilon_k \in \{0, 1\}$, *the corresponding iteration process converges to a unique attractor initialized with* $A \subset K^{n-1}$.

Remark 1. *The given modification mainly focuses on the case of* p^0 *being a* 4×3 *matrix. When* p^0 *is a* $n \times 3$ *matrix, a similar modification can be given.*

Now we modify the iterated function systems in Example 1 in several ways to derive different interesting attractors.

Example 2. *We keep the original* $\mathcal{F}_0^{[k]}$ *i.e.*

$$\mathcal{F}_0^{[k]} = \{f_{0,i}^{[k]}, i = 1, \cdots, 8\}$$

where the iterated functions $f_{0,i}^{[k]}$ $(i = 1, \cdots, 8)$ *are as in Equation (12). Besides, we give the modified iterated function systems*

$$\mathcal{F}_1^{[k]} = \{f_{1,3,0,0,0,0}^{[k]}, f_{1,4,0,-1,0,1}^{[k]}, f_{1,7,0,0,0,0}^{[k]}, f_{1,8,1,2,0,-1}^{[k]}\},$$
$$\bar{\mathcal{F}}_1^{[k]} = \{f_{1,2,0,1,0,-1}^{[k]}, f_{1,3,0,0,0,0}^{[k]}, f_{1,6,-1,-2,0,1}^{[k]}, f_{1,7,0,0,0,0}^{[k]}\}.$$

Then we have the new multiple function systems $\mathcal{F}_{\boldsymbol{\epsilon}}^{[k]} = \{\mathcal{F}_0^{[k]}, \mathcal{F}_1^{[k]}\}$ and $\bar{\mathcal{F}}_{\boldsymbol{\epsilon}}^{[k]} = \{\mathcal{F}_0^{[k]}, \bar{\mathcal{F}}_1^{[k]}\}$.

Figure 6 shows the sets with controlled asymmetry obtained using $\mathcal{F}_{\boldsymbol{\epsilon}}^{[k]}$ (left) and $\bar{\mathcal{F}}_{\boldsymbol{\epsilon}}^{[k]}$ (right) with $\boldsymbol{\epsilon} = (1, 1, 1, 0)$ for the given p^0 in Equation (11).

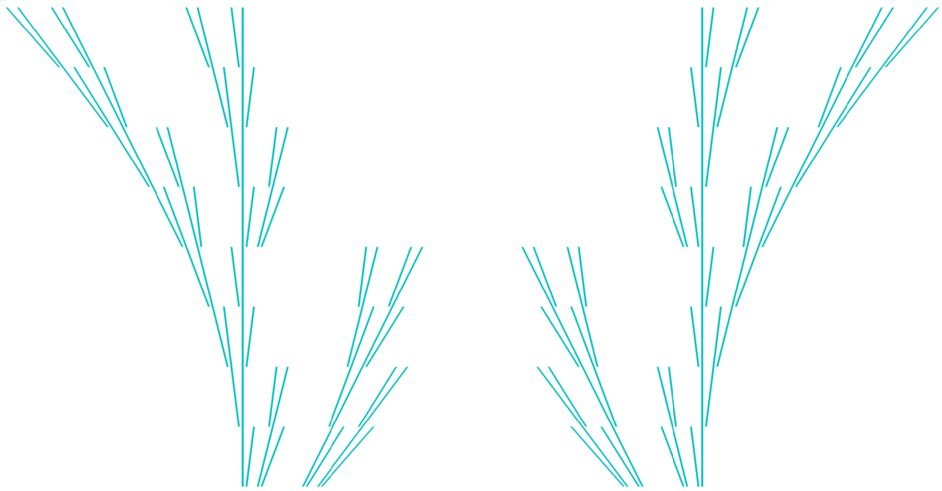

Figure 6. With p^0 in Equation (11), the sets obtained using $\mathcal{F}_{\boldsymbol{\epsilon}}^{[k]}$ (left) and $\bar{\mathcal{F}}_{\boldsymbol{\epsilon}}^{[k]}$ (right) with $\boldsymbol{\epsilon} = (1, 1, 1, 0)$.

Example 3. *Now we again modify* $\mathcal{F}_1^{[k]}$ *in Example* 1 *to get the new* $\mathcal{F}_1^{[k]} = \{f_{1,2,0,1,0,-1}^{[k]}, f_{1,3,0,0,0,0}^{[k]}, f_{1,4,0,-1,0,1}^{[k]}, f_{1,7,0,0,0,0}^{[k]}\}$ *while keeping* $\mathcal{F}_0^{[k]} = \{f_{0,i}^{[k]}, i = 1, \cdots, 8\}$*. Then we get a new multiple function system* $\mathcal{F}_{\boldsymbol{\epsilon}}^{[k]}$*. With the same* p^0 *in Equation (11), we get the set with controlled asymmetry shown in **Figure** 7.*

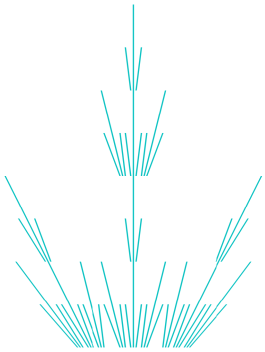

Figure 7. With p^0 in Equation (11), the set obtained using the new modified multiple function system with $\boldsymbol{\epsilon} = (1, 1, 1, 0)$.

Example 4. *Now we choose* $\mathcal{F}_0^{[k]} = \{f_{0,1}^{[k]}, f_{0,2}^{[k]}, f_{0,3}^{[k]}, f_{0,4}^{[k]}, f_{0,6}^{[k]}, f_{0,7}^{[k]}\}$ *and give the new* $\mathcal{F}_1^{[k]} = \{f_{1,1,0,0,0,0}^{[k]}, f_{1,2,0,0,0,0}^{[k]}, f_{1,3,0,0,0,0}^{[k]}, f_{1,4,0,0,0,0}^{[k]}, f_{1,6,2,3,0,-1}^{[k]}, f_{1,7,2,3,0,-1}^{[k]}\}$*. Then we get a new multiple function system* $\mathcal{F}_{\boldsymbol{\epsilon}}^{[k]}$*. **Figure 8** shows the sets generated using this new multiple function system with different* $\boldsymbol{\epsilon}$ *for the given* p^0 *in Equation (11).*

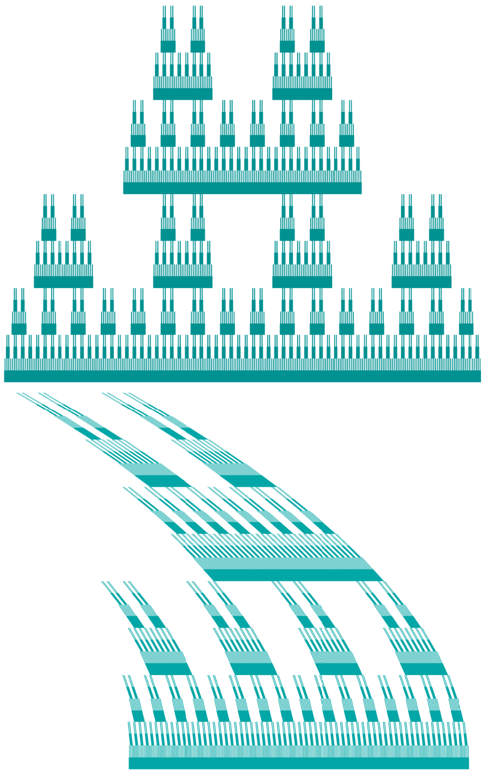

Figure 8. Sets generated using the new multiple function system with $\boldsymbol{\epsilon} = (0, 0, 0, 0, 0)$ (left) and $(1, 1, 1, 1, 0)$ (right) for the given p^0 in Equation (11).

4.3. Discussion on applications

Now we give a brief discussion on the applications of the new multiple function system.

Such a system can be used to simulate natural scenes. As pointed out in [11], fractals can be used to characterize the natural scenes. Yet, most of these fractals are actually isotropic ones, like the attractors generated by the L-systems. Unlike such fractals, the attractors in this paper possess directions and thus have controlled asymmetry. Therefore, they are more closer to nature. For example, the attractors in **Figures 6–7** can be seen as fractal trees. The attractors in **Figure 6** can be used to simulate the asymmetric growth of trees or grass caused by wind and the attractor in **Figure 7** simulates the growth of bamboo.

Apart from these fractal trees, the multiple function system approach can also be used to simulate other scenes like mountains used in animation. Besides the natural scenes, these directional attractors can also be used to simulate the blood circulation.

5. Conclusions

This paper introduced a new multiple function system derived from multiple subdivision schemes, establishing a novel link between anisotropic subdivision operators and fractals. Key contributions include: (1) a rigorous proof of the existence and convergence of path-dependent attractors for the proposed multiple function system, providing the framework to unify subdivision schemes with directional fractal generation; (2) two systematic control mechanisms, i.e., path selection and shear operator modulation—changing both the shearing operators and paths. These results quantitatively advance the understanding of structured fractals, offering tools for applications in procedural modeling and anisotropic pattern design. Yet, most of the existing multiple subdivision owns large determinant, leading to complexity issues when generating attractors with different directions. Therefore, future work will focus on designing new similar systems based on anisotropic subdivision operators with dilation matrices of small determinants and also implementing the corresponding systems in applications like natural scenes simulation.

Author contributions: Conceptualization, BZ and HZ; methodology, BZ; formal analysis, BZ and XY; writing-original draft preparation, BZ; writing-review and editing, HZ and XY. All authors have read and agreed to the published version of the manuscript.

Funding: This research is funded by Science Research Project of Hebei Education Department, NO. QN2024065 and the National Natural Science Foundation of China (12201453).

Conflict of interest: The authors declare no conflict of interest.

References

1. Schaefer S, Levin D, Goldman R. Subdivision schemes and attractors. In: Proceedings of the third Eurographics symposium on Geometry processing; 4–6 July 2005; Goslar, Germany.

2. Levin D, Dyn N, Puthan Veedu V. Non-stationary versions of fixed-point theory, with applications to fractals and subdivision. Journal of Fixed Point Theory and Applications. 2019; 21(1): 26.
3. Hu Y, Zheng H, Geng J. Calculation of dimensions of curves generated by subdivision schemes. International Journal of Computer Mathematics. 2019; 96(6): 1278–1291.
4. Dyn N, Levin D, Massopust P. Attractors of trees of maps and of sequences of maps between spaces with applications to subdivision. Journal of Fixed Point Theory and Applications. 2020; 22(1): 14.
5. Zheng H, Ye Z, Lei Y, et al. Fractal properties of interpolatory subdivision schemes and their application in fractal generation. Chaos, Solitons & Fractals. 2007; 32(1): 113–123.
6. Goldman R. The fractal nature of Bezier curves. In: Proceedings of the Geometric Modeling and Processing 2004; 13–15 April 2004; Washington, DC, USA. pp.3–11.
7. Ghaffar A, Javed S, Mustafa G, et al. Generation of fractal curves using new binary 8-point interpolatory subdivision scheme. Applied Mathematics in Science and Engineering. 2024; 32(1): 2367718.
8. Bruni V, Pelosi F, Vitulano D. Fractal properties of 4-point interpolatory subdivision schemes and wavelet scattering transform for signal classification. Applied Numerical Mathematics. 2025; 208: 256–270.
9. Yao S, Ashraf P, Ghaffar A, et al. Fractal And Convexity Analysis Of The Quaternary Four-Point Scheme And Its Applications. Fractals. 2023; 31(10): 2340088.
10. Vijay, Saravana Kumar G, Chand AKB. A comprehensive discussion on various methods of generating fractal-like Bézier curves. Computational and Applied Mathematics. 2024; 43(6): 368.
11. Pentland AP. Fractal-based description of natural scenes. IEEE Transcations on Pattern Analysis and Machine Intelligence. 1984; 6: 661–674.
12. Wolski M, Podsiadlo P, Stachowiak GW. Directional fractal signature analysis of self-structured surface textures. Tribology Letters. 2012; 47(3): 323–340.
13. Wolski M, Podsiadlo P, Stachowiak GW. Directional fractal signature analysis of trabecular bone: evaluation of different methods to detect early osteoarthritis in knee radiographs. Proceedings of the Institution of Mechanical Engineers, Part H: Journal of Engineering in Medicine. 2009; 223(2): 211–236.
14. Wu J. Analyses and simulation of anisotropic fractal surfaces. Chaos, Solitons and Fractals. 2002; 13: 1791–1806.
15. Wu J, He F, Li S. Generalized fixed-point theorem for strict almost ϕ-contractions with binary relations in b-metric spaces and its application to fractional differential equations. Advances in Differential Equations and Control Processes. 2025; 32: 2510.
16. Arora S, Mebrek-Oudina F, Sahani S. Super convergence analysis of fully discrete Hermite splines to simulate wave behaviour of Kuramoto–Sivashinsky equation. Wave Motion. 2023; 121: 103187.
17. Priyanka P, Mebarek-Oudina F, Sahani S, et al. Travelling wave solution of fourth order reaction diffusion equation using hybrid quintic hermite splines collocation technique. Arabian Journal of Mathematics. 2024; 13(2): 341–367.
18. Kutyniok G, Sauer T. Adaptive directional subdivision schemes and shearlet multiresolution analysis. SIAM Journal on Mathematical Analysis. 2009; 41: 1436–1471.
19. Sauer T. Shearlet Multiresolution and Multiple Refinement. In: Kutyniok G, Labate D (editors). Shearlets. Springer; 2011.
20. Cotronei M, Rossini M, Sauer T, et al. Filters for anisotropic wavelet decompositions. Journal of Computational and Applied Mathematics. 2019; 349: 316–330.
21. Rossini M, Volonte E. On directional scaling matrices in dimension $d = 2$. Mathematics and Computers in Simulation. 2018; 147: 237–249.
22. Zhang B, Zheng H, Chen Y. Multiple-Function Systems Based on Regular Subdivision. Fractal and Fractional. 2022; 6(11): 677.
23. Jia RQ. Approximation properties of multivariate wavelets. Mathematics of Computation. 1998; 67: 647–665.
24. Barlow MT, Hambly BM. Transition density estimates for Brownian motion on scale irregular Sierpinski gaskets. Annales de I'institut Henri Poincare(B) Probability and Statistics. 1997; 33: 531–557.